

Ongoing Development of a 3D Printed Four-Stage In Vitro Fracture Callus Model

Nicholas Lamb^{1,2}, Sophia Sangiorgio^{1,2}, Eddie Ebramzadeh^{1,2}, Sang-Hyun Park^{1,2}

1: University of California Los Angeles Department of Bioengineering, Los Angeles, USA

2: The J. Vernon Luck, Sr. Orthopaedic Research Center at Lusk Orthopaedic Institute for Children, Los Angeles, USA

Contact Email: Nlamb@mednet.ucla.edu

Introduction

Current models to study fracture fixation devices are limited to time zero models and do not include or simulate local structural changes due to biological healing. Prior studies have used models ranging in sophistication from layers of duct tape to particle laden polyurethane resins.¹⁻³ While they do provide valuable information, the methods used in these studies have issues with efficacy, cost, and/or reproducibility. Particularly, these models all have consistent material properties throughout their entire “callus” structure, which is inconsistent with natural fracture callus formation. Without an accurate, reproducible in vitro model, alternatives for early-stage testing of fracture fixation devices include in silico, cadaveric, or animal models. Each of which has concerns regarding cost, ethics, and/or accuracy. Previous studies have used advances in 3D-printing technology to create biomimetic models of bones made from polylactic acid (PLA).⁴⁻⁷ Tensile and torsional properties of PLA were previously examined in our lab⁵, and this work expands on bending properties of PLA as well as the tensile properties of a more elastic material, thermoplastic elastomer 95A (TPU). Using the material properties found in this study, 3D printing technology can be utilized in a similar fashion to create models for mimicking the varied material properties throughout fracture callus tissue. In summary, the goal of the study was to quantify important mechanical properties of a matrix of combinations of infill densities and patterns to develop a prototype of a four-stage fracture callus model.

Methods

The two materials tested for use as localized regions in the fracture callus models were PLA and TPU. Both materials were evaluated in the triangle, zig-zag, and gyroid infill patterns under the following infill densities: 100%, 80%, 60%, 45%, 30%, 25%, and 20%. The evaluations followed ASTM standards D5279, D412, D790, and D695. Five specimen, printed with an Ultimaker S5 3D printer, were printed for each group. Specimen for the tensile and bending tests were printed in specific orientations to match the appropriate loading direction that would be experienced by fracture callus tissue. The measured mechanical properties were then compared to in literature values for callus material properties shown in table 1. Additionally, several prototypes in full PLA and full TPU have been printed and attached to a simulated fracture gap on synthetic model tibias made by Sawbones (Vashon, Wa) using epoxy resin with similar mechanical properties to the cortical shell of Sawbones long bone models.

Results

Minimal differences in effective elastic modulus were found between the 20% and 25% infill densities for TPU specimen, but the other infill percentages had near linear increases ($R^2=0.99, 0.98, \text{ and } 0.99$ for triangle zig-zag, and gyroid respectively). The zig-zag pattern infills had the sharpest increase in modulus, followed by the gyroid, and then the triangle patterns. When TPU prints were separated by infill pattern, there were significant differences between zig-zag, triangle, and gyroid patterns at all infill densities ($p < 0.01$), except the 60% and 80% groups. The elastic modulus of the TPU specimen ranged between 9.16 and 90.7 MPa for zig-zag pattern, 7.66 and 72.5 MPa for triangle, and 14.7 and 89.4 MPa for gyroid. The bending modulus of PLA exhibited exponential growth for all infill patterns ($R^2=0.98, 0.99, \text{ and } 0.99$ for triangle zig-zag, and gyroid respectively). When separated by infill pattern, there were significant differences between all patterns at all infill densities, excepting the triangle and gyroid infill patterns with 30 and 45% infill densities. The bending modulus for PLA specimen ranged between 22.3 and 2887 MPa for zig-zag, 102 and 2209 MPa for triangle, and 150 and 3161 MPa for gyroid.

Discussion

As expected, in general, increasing infill density of the printed structure effectively increases stiffness. Results with PLA infill patterns, from this work and previous work by Wahbeh et al, found significant differences between all three infill patterns; however, data from lower infill density TPU specimen had issues with creating strong connection points at key locations along the exterior walls in the slicer program. This issue is dependent on the geometry and size of printed specimen and may be mitigated by including an exterior shell structure in the model, but at lower print infills should be monitored while slicing the CAD model in preparation for printing. Ultimately, alteration of infill density with careful selection of infill pattern can alter local stiffness properties throughout 3D printed structures. The brittleness of PLA limits its use for early stages of fracture healing, but these phases may be well represented by the less stiff but more ductile TPU. Further testing of full-scale models will be necessary to evaluate if full PLA and full TPU models can be representative of different physiological healing stages or if combinations of both materials may be best representative for each stage.

Significance

Modification of infill density and pattern can effectively be used to create localized zones within our fracture callus model. The mechanical properties observed in both PLA and TPU models fit within the range of fracture callus mechanical properties. PLA, TPU, and PLA/TPU composites have potential for modeling stages of fracture callus development. The successful development of a 3D printed fracture callus model would provide a more cost effective and ethical method for early-stage testing of innovative fracture fixation devices.

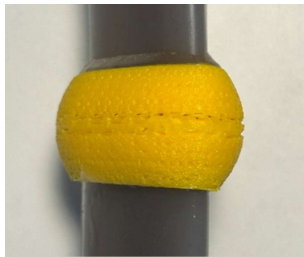


Figure 1: Prototype model of a simulated mid-shaft transverse tibial fracture using a Sawbones

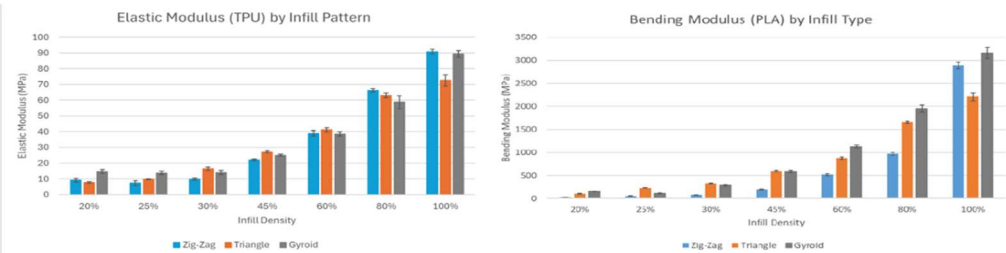


Figure 2: Elastic modulus of TPU (left) and bending modulus of PLA (right) separated by infill density and infill pattern.

Table 1: Callus material properties from published sources^{2, 8-20}

Stage of Healing	Inflammatory Phase	Callus Formation	Ossification	Remodelling
Elastic Modulus (MPa)	0.2-1.4	2-28	538-6000	10,000-20,000
Bending Stiffness (% intact)	< 5%	5% - 50%	50% - 95%	> 95%

References:

1. Faroug R, McCarthy I, Meswania J, Janna S, Wilson D, Taylor S. Strain response of an instrumented intramedullary nail to three-point bending. *J Med Eng Technol*. 2011 Jul;35(5):275-82.
2. Lacroix D, Prendergast PJ. A mechano-regulation model for tissue differentiation during fracture healing: analysis of gap size and loading. *J Biomech*. 2002 Sep;35(9):1163-71.
3. Mattei L, Di Puccio F, Marchetti S. In vivo impact testing on a lengthened femur with external fixation: a future option for the non-invasive monitoring of fracture healing? *J R Soc Interface*. 2018 May;15(142).
4. Bohl MA, Morgan CD, Mooney MA, Repp GJ, Lehrman JN, Kelly BP, et al. Biomechanical Testing of a 3D-printed L5 Vertebral Body Model. *Cureus*. 2019 Jan 15;11(1):e3893. Epub 20190115.
5. Wahbeh JM, Hookasian E, Lama J, Alam L, Park SH, Sangiorgio SN, et al. An additively manufactured model for preclinical testing of cervical devices. *JOR Spine*. 2024 Mar;7(1):e1285. Epub 20231006.
6. Wei F, Li Z, Liu Z, Liu X, Jiang L, Yu M, et al. Upper cervical spine reconstruction using customized 3D-printed vertebral body in 9 patients with primary tumors involving C2. *Ann Transl Med*. 2020 Mar;8(6):332.
7. Xu N, Wei F, Liu X, Jiang L, Cai H, Li Z, et al. Reconstruction of the Upper Cervical Spine Using a Personalized 3D-Printed Vertebral Body in an Adolescent With Ewing Sarcoma. *Spine (Phila Pa 1976)*. 2016 Jan;41(1):E50-4.
8. Claes LE, Heigele CA. Magnitudes of local stress and strain along bony surfaces predict the course and type of fracture healing. *J Biomech*. 1999 Mar;32(3):255-66.
9. Comiskey DP, Macdonald BJ, McCartney WT, Synnott K, O'Byrne J. The role of interfragmentary strain on the rate of bone healing—a new interpretation and mathematical model. *J Biomech*. 2010 Oct 19;43(14):2830-4. Epub 20100723.
10. Steiner M, Claes L, Ignatius A, Simon U, Wehner T. Numerical simulation of callus healing for optimization of fracture fixation stiffness. *PLoS One*. 2014;9(7):e101370. Epub 20140703.
11. Steiner M, Volkheimer D, Meyers N, Wehner T, Wilke HJ, Claes L, et al. Comparison between different methods for biomechanical assessment of ex vivo fracture callus stiffness in small animal bone healing studies. *PLoS One*. 2015;10(3):e0119603. Epub 20150317.
12. Augat P, Burger J, Schorlemmer S, Henke T, Peraus M, Claes L. Shear movement at the fracture site delays healing in a diaphyseal fracture model. *J Orthop Res*. 2003 Nov;21(6):1011-7.
13. Augat P, Margevicius K, Simon J, Wolf S, Suger G, Claes L. Local tissue properties in bone healing: influence of size and stability of the osteotomy gap. *J Orthop Res*. 1998 Jul;16(4):475-81.
14. Augat P, Merk J, Genant HK, Claes L. Quantitative assessment of experimental fracture repair by peripheral computed tomography. *Calcif Tissue Int*. 1997 Feb;60(2):194-9.
15. Augat P, Merk J, Ignatius A, Margevicius K, Bauer G, Rosenbaum D, et al. Early, full weightbearing with flexible fixation delays fracture healing. *Clin Orthop Relat Res*. 1996 Jul(328):194-202.
16. Augat P, Penzkofer R, Nolte A, Maier M, Panzer S, v Oldenburg G, et al. Interfragmentary movement in diaphyseal tibia fractures fixed with locked intramedullary nails. *J Orthop Trauma*. 2008 Jan;22(1):30-6.
17. Tiedeman JJ, Lippiello L, Connolly JF, Strates BS. Quantitative roentgenographic densitometry for assessing fracture healing. *Clin Orthop Relat Res*. 1990 Apr(253):279-86.
18. Wehner T, Gruchenberg K, Bindl R, Recknagel S, Steiner M, Ignatius A, et al. Temporal delimitation of the healing phases via monitoring of fracture callus stiffness in rats. *J Orthop Res*. 2014 Dec;32(12):1589-95. Epub 20140902.
19. Wehner T, Steiner M, Ignatius A, Claes L. Prediction of the time course of callus stiffness as a function of mechanical parameters in experimental rat fracture healing studies—a numerical study. *PLoS One*. 2014;9(12):e115695. Epub 20141222.
20. Claes LE, Cunningham JL. Monitoring the mechanical properties of healing bone. *Clin Orthop Relat Res*. 2009 Aug;467(8):1964-71. Epub 20090226.